Journal of Cellular Biochemistry 53:360–372 (1993)

Modulation of Human Microvascular Endothelial Cell Bioenergetic Status and Glutathione Levels During Proliferative and Differentiated Growth

S.R. Mallery, L.E. Lantry, H.B. Laufman, R.E. Stephens, and G.P. Brierley

Departments of Pathology (S.R.M., L.E.L., R.E.S.), and Medical Biochemistry (G.P.B.) and Comprehensive Cancer Center (H.B.L.), Colleges of Medicine and Dentistry, Ohio State University, Columbus, Ohio

Abstract *During* angiogenesis, formerly differentiated human microvascular endothelial cells (HMECs) return to a proliferative growth state. Many fundamental questions regarding HMEC function, such as how HMECs adapt to changes in bioenergetic requirements upon return to proliferative growth, remained unanswered. In this study, we evaluated whether modifications in HMEC bioenergetic profiles and glutathione (GSH) levels accompanied the cellular transition between differentiated and proliferative growth. To provide insight into the continuum of cellular adaptations that occur during this transition, we used a method recently developed in our laboratory that induces a state of morphological and functional predifferentiation in HMECs. Cellular morphology, in conjunction with flow cytometric DNA analyses and HMEC functional assays (the directed migration and intercellular association involved in microtubule formation) were employed to validate the HMEC culture state of growth. Analysis of the HPLC nucleotide profiles disclosed several findings common to all culture growth states. These uniform findings, e.g., cellular energy charges >0.90, and highly reduced redox states, revealed that cultured HMECs maintain high rates of oxidative metabolism. However, there were also significant, culture growth state related differences in the nucleotide profiles. Proliferative HMECs were shown to possess significantly higher (relative to both large vessel endothelial cells, and differentiated HMECs) levels of GSH and specific nucleotides which were related with a return to the active cell cycle-ATP, GTP, UTP, and CTP, and NADPH. Further, the nucleotide profiles and GSH levels of the predifferentiated HMECs were determined to be intermediate between levels obtained for the proliferative and differentiated HMECs. The results of this study demonstrate that the capacity to modulate their cellular bioenergetic status during growth state transitions is one of the adaptations that enable HMECs to retain a growth state reciprocity. In addition, our findings also show that HMECs, especially during the proliferative growth state, are biochemically distinct from endothelial cells harvested from large vessels, and therefore suggest that HMECs are the cells of choice to employ when studying diseases that affect the human microvasculature.

Key words: nucleotides, cell cycle, redox state, energy charge, cytoprotection, extracellular matrix, adhesion molecules

In addition to their well recognized role as conduits for blood-borne products, endothelial cells participate in many other functions, which include immunological interactions (by expression of specific adhesion molecules such as the endothelial leukocyte adhesion molecule [ELAM-1]), phagocytosis and modification of low density lipoproteins, and response to angiogenic stimuli by migration, proliferation, and neovascularization [2,12,43,46,50]. This diversity in endothelial cell function is possible due to both an inherent plasticity in the endothelial cell phenotype and a heterogeneity amongst endothelial cell populations [5,12]. Microvascular endothelial cells (MECs) are a specialized population of endothelial cells that share some characteristics with large vessel endothelial cells, but also possess some unique cellular features [5,12,28]. Because the microvasculature functions as the primary site for tissue perfusion, nutrient exchange, and cellular adhesions, MECs face stringent physiological and environmental pressures [3,4,9,13]. However, experimental and in vivo evidence suggests that MECs have the capacity to readily adapt to changes in their microenvironment [4,8,23,24,35]. The release during wound healing of angiogenic factors is one such environmental modulation that necessitates an MEC response [14,15,27,32]. Because MECs retain a

Received June 21, 1993; accepted August 6, 1993.

Address reprint requests to Susan R. Mallery, D.D.S., Ph.D., 305 W 12th Ave, #172, Postle Hall, College of Dentistry, Ohio State University, Columbus, OH.

growth state reciprocity, differentiated MECs can re-enter a proliferative growth state and therefore respond to the need for neovascularization [4,33].

Due to overlap in their physiological roles, both proliferative and differentiated MECs share some cellular needs inclusive of (1) cytoprotection, (2) sustained protein synthesis for cellular metabolism and extracellular matrix (ECM) formation and maintenance, and (3) the capacity to modify adhesion receptor expression/and or organization [1,4,12,15]. Further, because MECs function as the primary site for blood-tissue exchange, MECs are continually exposed to potential cytotoxic entities such as lipid peroxides and reactive oxygen species [4,48]. Therefore, cytoprotection is key for MEC survival [4,48]. Cytoprotection is one of the many cellular functions of glutathione (GSH, glutamycysteinylglycine) [38,39]. GSH, which is the primary intracellular free thiol, participates in many cellular roles inclusive of the inactivation of reactive oxygen species, (GSH peroxidase), detoxification of xenobiotics (GSH-S transferases), and the provision of reducing equivalents and maintenance of thiol dependent enzymatic activity (GSH and glutaredoxin) [21,38,39]. Numerous publications have focused on the importance of GSH's contribution in both cellular protection and cell cycle kinetics [6,30,34,37,45]. Although the microvasculature is a site where the presence of GSH would be beneficial, to our knowledge, there are no publications that report levels of GSH in human MECs (HMECs) during either proliferative or differentiated growth.

The return of formerly differentiated HMECs to the active cell cycle is accompanied by an alteration in cellular bioenergetic requirements [10,19,42]. Because during S, the DNA synthesis phase of the cell cycle, there are increased demands for both high energy phosphates and reducing equivalents, there are likely modifications in the HMEC bioenergetic profiles and GSH levels as HMECs re-enter the cell cycle [42]. However, due to the difficulties encountered in the isolation and culture of human MECs (HMECs), there is currently a deficit in the knowledge regarding many fundamental aspects of these cells. Information regarding the response of the HMEC bioenergetic status during the differentiated to proliferative growth transition would facilitate understanding how HMECs are able to modify their growth state in accordance with environmental demands.

In earlier studies, we have reported on the importance of an intracellular parameter, the cellular thiol redox status, on the regulation of cell cycle progression [34]. Relevant to this current study, it was found that normal human fibroblasts modify their GSH levels and redox state during the cell cycle [34]. Recently, we reported findings that demonstrated a rapidly inducible modification in HMEC phenotype and function in response to changes in the HMEC milieu [35]. In this recent study, it was shown that selective HMEC culture modifications, which caused an alteration in the HMEC-ECM interaction, resulted in the induction of a functional state of predifferentiation in HMECs [35].

This current study reports for the first time the bioenergetic status and GSH levels of cultured human microvascular endothelial cells. In this study, we evaluated whether modifications in HMEC bioenergetic profiles and GSH levels accompanied the cellular transition between differentiated and proliferative growth. Further, we incorporated the determination of predifferentiated HMEC GSH levels and bioenergetic profiles into this study to facilitate the determination of the continuum of cellular adaptations that occur during the differentiated-proliferative transition. In this paper, we report results that demonstrate that HMECs significantly modify both their bioenergetic profiles and GSH levels during their differentiated-proliferative growth transition.

MATERIALS AND METHODS

Isolation and Characterization of HMECs

The endothelium of the choriocapillaris was specifically chosen as the source of HMECs for this work for several reasons. First, the incidence of ocular vascular pathology, e.g., diabetic proliferative retinopathy, suggests that this component of the microvasculature is susceptible to environmental influences [47]. Further, due to its unique location, this microvascular bed can be easily separated from the possible contaminating cells (pericytes and retinal pigmented epithelial cells), prior to primary culture, yielding greater that 98% pure HMEC cultures [7,29].

Fresh human eyes, ranging in age from 14 to 74 years, were obtained from the Lions Eye Bank, or directly from The Ohio State University Hospitals, and processed within 10 h postmortem. Excess muscle and fat was removed, the eyes dipped in 95% EtOH, followed by two changes of phosphate buffered saline (PBS) with

500 μg/ml penicillin, 500 μg/ml streptomycin, and 10 μg/ml amphotericin B. A circumferential incision was made and the anterior chamber was removed. The retina was then drawn into a pipette, and released with fine scissors for further processing.

The RPE layer was removed by a modification of standard methods [29], with 1 U/ml dispase (Boehringer Mannheim), at 37°C for 30 min, followed by gently trituration. After washing with PBS to remove the RPE layer, as well as any remaining dispase, a 1 mm margin was cut around the remnants of the optic nerve and peripapillary area. The choroid was then teased away from the sclera with fine forceps for further processing.

The digestion buffer consisted of PBS with 1 mg/ml bovine serum albumin (BSA) (Sigma), 0.5 mg/ml each of collagenase type I (Worthington), and II (Boehringer-Mannheim). Tissue was briefly cross-blade minced, and transferred to a shaker flask for a 30 to 60 min digestion at 37°C, in a shaking water bath. The digest was triturated and diluted 10-fold with PBS, and layered onto a 5% BSA gradient, at unit gravity for 30 min. The middle zone was collected and centrifuged for 5 min at 800 rpm.

The pellet was resuspended in endothelial cell growth medium consisting of M-199 (GIBCO), completed with 15 mM HEPES, 90 μg/ml Na-heparin, 150 μg/ml endothelial cell growth supplement (ECGS, prepared in-house), and 10% fetal bovine serum (Hyclone) (ENDO-C). The isolate was then plated onto human fibronectin-coated (25 μg/ml, hFN), 6-well tissue culture plates, and incubated at 37°C, 5% CO_2, for 5–7 days without disturbing the plate. After this period, the wells were inspected for colonies, and the medium was replaced with fresh ENDO-C.

Endothelial colonies were readily identified by morphology in most primary cultures, which allowed for selective removal of any remaining contamination cell types (pericytes). Nonendothelial colonies, and individual cells were removed by vacuuming.

Identification of HMECs has been based upon morphological characteristics, expression of specific adhesion receptor molecules, and spontaneous formation of tubules in culture [8]. Our HMECs have been identified as endothelial in origin by Dil-Ac-LDL uptake, with standard methods [Voyta et al., 1984], using human umbilical vein endothelial cells as the positive control, and human normal dermal fibroblasts as a negative control [50]. In addition, cultures were shown to have positive staining for ELAM-1 [5], after induction by TNF-a. Within 14 to 21 days after achieving contact inhibition, our HMEC cultures demonstrated the spontaneous formation of microtubules [8]. These cultures have also been screened for the absence of epithelial cytokeratins using a pan-keratin monoclonal antibody (Hybritech). The antibody HMB45 (DAKO), was used to determine the absence of any melanin-producing capability. Finally, cultures were shown to be nonpericyte by standard immunocytochemistry for smooth muscle-specific alpha actin (Sigma).

Modulation of HMEC Growth State

Cultures of HMECs were permitted to achieve spontaneous differentiation by employing methods reported by Ingber and Folkman, 1989 [24]. HMEC cultures were permitted to achieve contact inhibition, and fed approximately one-third fresh media to the two-thirds conditioned media every fourth day. Within 14 to 21 days after reaching contact inhibition, the appearance of microtubules in the cultures was noted.

Cultures of HMECs were also induced to enter a predifferentiated growth state, by methods reported in our recent publication [35]. Briefly, HMECs were cultured for 48 h in a low serum (0.3% FBS) M-199 medium that contained a final concentration of 4 mM ethionine (Sigma Chemical Co., St. Louis, MO).

Validation of HMEC growth state was determined by the use of three parameters-cellular morphology [23,24], functional assays (directed migration and intercellular association) [35], and flow cytometric DNA analyses.

Determination of Total Cellular GSH

After harvesting and centrifugation, the cell pellet was resuspended to a volume of 0.5 ml in 4 mM EDTA-PBS for number and viability (trypan blue exclusion) quantification. Proteins were precipitated via addition of an equal volume of 2M perchloric acid (PCA). The samples were stored at −20°C. Twelve hours or less prior to assay, the supernates were neutralized to pH 6.02 (using 2M KOH + 0.4 M morpholineethanesulfonic acid (MES), (Sigma Chemical Co., St. Louis, MO), and frozen overnight.

Cell pellets from samples used in GSSG determination were resuspended to 1 ml in ice cold 1 M PCA, 1 mM EDTA, 0.02 M NEM (N-ethylmalemide, Sigma Chemical Co., St. Louis, MO).

Samples were stored at −20°C. Twelve hours or less prior to the assay, the samples were thawed, 1 ml of 1.3 M K_2HPO_4 was added, samples were stirred for 30 min, and then centrifuged to pellet the $KClO_4$ salt. The NEM contained in the GSSG samples (which were kept on ice during the extraction) was removed by 5 extractions, using a 2-fold excess of ice-cold, H_2O-saturated ethyl acetate. A light stream of N_2 gas was used to remove any residual ethyl acetate, and the samples stored at −20°C overnight. For control purposes, the GSSG standards underwent the same ethyl acetate extraction as the GSSG samples.

Cellular levels of total GSH (GSH, and the disulfide, GSSG) were determined according to the method of Eyer and Podhradsky [11]. NADPH, GSH, GSSG, glutathione reductase (GR) (Type IV), and DTNB were obtained from Sigma. The enzymatic kinetics in the Eyer assay have been modified so that the GR catalyzed step is no longer rate limiting. Therefore, this method is much less susceptible to any endogenous, intrasample GR inhibitors [41].

Rapid reaction kinetics were followed on a SLM-AMINCO DW 2C dual wavelength spectrophotometer, with the following instrument settings: 412 nm vs. 550 nm, 3 nm bandwidth, 0.05 Abs, 50 sec/in. Sample concentrations (nmol/ml) were determined by comparison with a 10-point standard curve conducted concurrently. The GSH standard curve ranged from 0.2 nmol/ml to 2 nmol/ml; the GSSG standards ranged from 0.125 nmol/ml to 1.5 nmol/ml. Both the GSH and the GSSG standard curves were linear over their entire range, and results were expressed as GSH or GSSG/mg protein.

Determination of Cellular Bioenergetic Status and Redox Poise [ratio NAD(P)H/NAD(P)]

Cellular levels of nucleotides and nucleosides were determined by high performance liquid chromatography (HPLC) by a modification the method of Harsem et al. [1982] [18].

Cells were harvested, washed twice with PBS, and resuspended in 500 μl of serum-free medium. Cellular extraction were conducted in chilled microfuge tubes that contained a bottom layer of 100 μl of 2 M perchloric acid (PCA) with an overlying organic layer comprised of 500 μl of 93% bromododecane (BDD), and 7% dodecane (DD). The cell samples were gently layered over the ice cold BDD/DD/PCA, centrifuged for 1 min at 15,000 rpm, and the top aqueous phase removed with a pasteur pipette. A cotton swab was used to remove the BDD/DD, and clean the sides of the tube. The cellular pellet was dispersed by addition of 200 μl, ice-cold H_2O, followed by vigorous vortexing. The resuspended cellular extracts were kept on ice for 10 min, and then centrifuged for 1 min at 15,000 rpm. The PCA extract was the transferred to another cold microfuge tube, and 500 μl of freshly prepared, ice cold, 4:1 freon:trioctylamine was added to extract the lipids, and to neutralize the PCA. The sample was vortexed at maximum speed for 30 s, and then centrifuged for 1 min at 15,000 rpm. The clear, aqueous layer was removed, added to an equivalent volume of ice cold H_2O, and stored at −20°C until injected onto the HPLC column.

Chromatography

Adenine, nicotinamide nucleotides, and respective nucleosides were separated on a Partisil 10 SAX column (Whatman) using a phosphate and pH gradient [17]. Buffers were prepared fresh on the day of use, filtered through a 0.2 μM Millipore membrane filter, and degassed by helium spargling. Buffer A consisted of 0.01 M H_3PO_4, pH 2.65, buffer B was 0.75 M KH_2PO_4, pH 4.5, with detection at 254 nm. Because reduced nicotinamide nucleotides undergo degradation during acid extraction, PCA exposed NADH and NADPH standards were used to determine the position of the reduced nicotinamide nucleotide degradatory fragments. Notably, both the NADH and NADPH peaks separated at distinct sites from other peaks, and the area under the NADH and NADPH peaks remained constant during varying lengths of PCA exposure [20].

On many of the cellular samples, the UTP and CTP peaks co-eluted. Therefore, the levels of these high energy phosphates are expressed as UTP and CTP.

Protein Determination

Cellular protein levels were determined by the Lowry method, using bovine gamma globulins as the standard protein [31]. To remove any residual BDD/DD, the nucleotide protein samples were washed twice in acetone and given a 4 min, 15,000 rpm centrifuge step after each wash. To determine if the BDD/DD separation and the acetone washing affected the sample protein content, or its optical density, bovine gamma globulin standards were centrifuged

through BDD/DD, and washed twice with acetone. Comparison of the optical densities obtained between treated and nontreated bovine gamma globulin standards demonstrated that the acetone wash did not affect optical densities, nor did it cause protein loss.

HMEC Nuclei Isolation, Staining, and Flow Cytometry

Nuclei were isolated in accordance with the method of Pollack, 1990 [44]. After harvesting, the HMECs were washed with PBS, and then resuspended in 1 ml of ice cold nuclear isolation buffer (0.5% Nonidet P-40, 0.05 M NaCl, 1.0 mM EDTA, 0.05 M Trizma base:HCl, pH 7.4), and vortexed at maximum speed for 5 s. Then, 2 ml of 0.03 M $NaHCO_3$ and 12 ml of PBS-0.02% EDTA were added, and the nuclei centrifuged at 4°C, 1,000*g* for 10 min. The supernate was carefully removed, and the nuclear pellet was resuspended in 2 ml PBS-0.02% EDTA, followed by 0.8 ml of 4% formaldehyde. The sample was mixed well, and stored at 4°C until awaiting staining with propidium iodide (PI).

Prior to DNA staining, RNA was removed by treating the nuclei with 150 U/ml of RNAase (RNAase A, Worthington Biochemicals, Freehold, NJ), for 20 min at 37°C. DNA was stained by suspending the nuclear preparation in 50 μg/ml PI (Sigma), and incubated overnight at 4°C.

The propidium iodide stained nuclei were analyzed on an Epics ELITE flow cytometer (Coulter Electronics, Inc. Hialeah, FL). The excitation beam, 12 mW from the 488 nm line of the air-cooled argon laser (Cyonics), was focused through a 8 mm × 80 mm beamshaper lens (Coulter 6604660). The pulse area and peak of the PI emission were collected through a 488 long pass dichroic, a 488 blocker filter, and finally a 550 long pass dichroic and then plotted as the abscissa and ordinate of a cytogram. A logic gate region was drawn on this cytogram to exclude doublet and higher order aggregate events from analysis. At least 5,000, but usually 20,000, events of interest were collected.

The histograms were processed with the cell cycle analysis software MULTICYCLE, (Phoenix Flow Systems). Debris background was calculated and subtracted.

RESULTS

Preliminary studies, conducted to evaluate HMEC growth properties, showed that HMEC morphology is markedly affected by the culture growth state (Fig. 1). Proliferative HMECs possess a nonpolar, cobblestone morphology, and contain numerous mitotic figures. In contrast, differentiated HMECs have a polar, elongated phenotype and demonstrate spontaneous formation of microtubules. These initial growth characterization studies also demonstrated that HMECs not only show a reciprocity between proliferative and differentiated growth, but also that this growth state transition occurs in an expeditious fashion. Within hours after return to noncontact inhibited growth state, differentiated HMEC cultures returned to proliferative growth (Fig. 2).

Although the proliferative and differentiated HMEC cultures possessed distinctive light microscopic appearances, flow cytometric DNA analyses were conducted to confirm the culture state of growth. The cell cycle distributions determined by flow cytometric DNA analyses were congruent with the HMEC light microscopic appearance (Fig. 3). While the DNA profiles of proliferative HMECs demonstrated ongoing cell cycle progression, the differentiated HMEC histograms revealed that differentiated HMECs were in a quiescent growth state, with $\geq 84\%$ of the differentiated cultures in the G0/G1 phase of the cell cycle. These findings, in conjunction with the HMEC microscopic appearance and functional assay responses [35], confirmed that the proliferative and differentiated cultures were in active or quiescent growth states, respectively. Biochemical studies were also conducted on a third culture group, HMECs that were cultured in a low serum, ethionine containing medium. Previously, we have shown that this protocol results in induction of a state of phenotypic and functional predifferentiation in HMECs [35].

Studies were conducted to determine if human endothelial cells isolated from other sites (large vessel-human umbilical endothelial vein) also possessed a growth state reciprocity. Results of initial studies showed that in contrast to HMECs, human endothelial vein endothelial cells (HUVECs) were not capable of undergoing differentiation under the same culture conditions that induced differentiation in HMECs. Failure to pass HUVEC cultures within 24 h after culture confluence resulted in a marked loss of cellular attachment and viability. Within 72 h after reaching contact inhibition, there was complete loss of the HUVEC cultures.

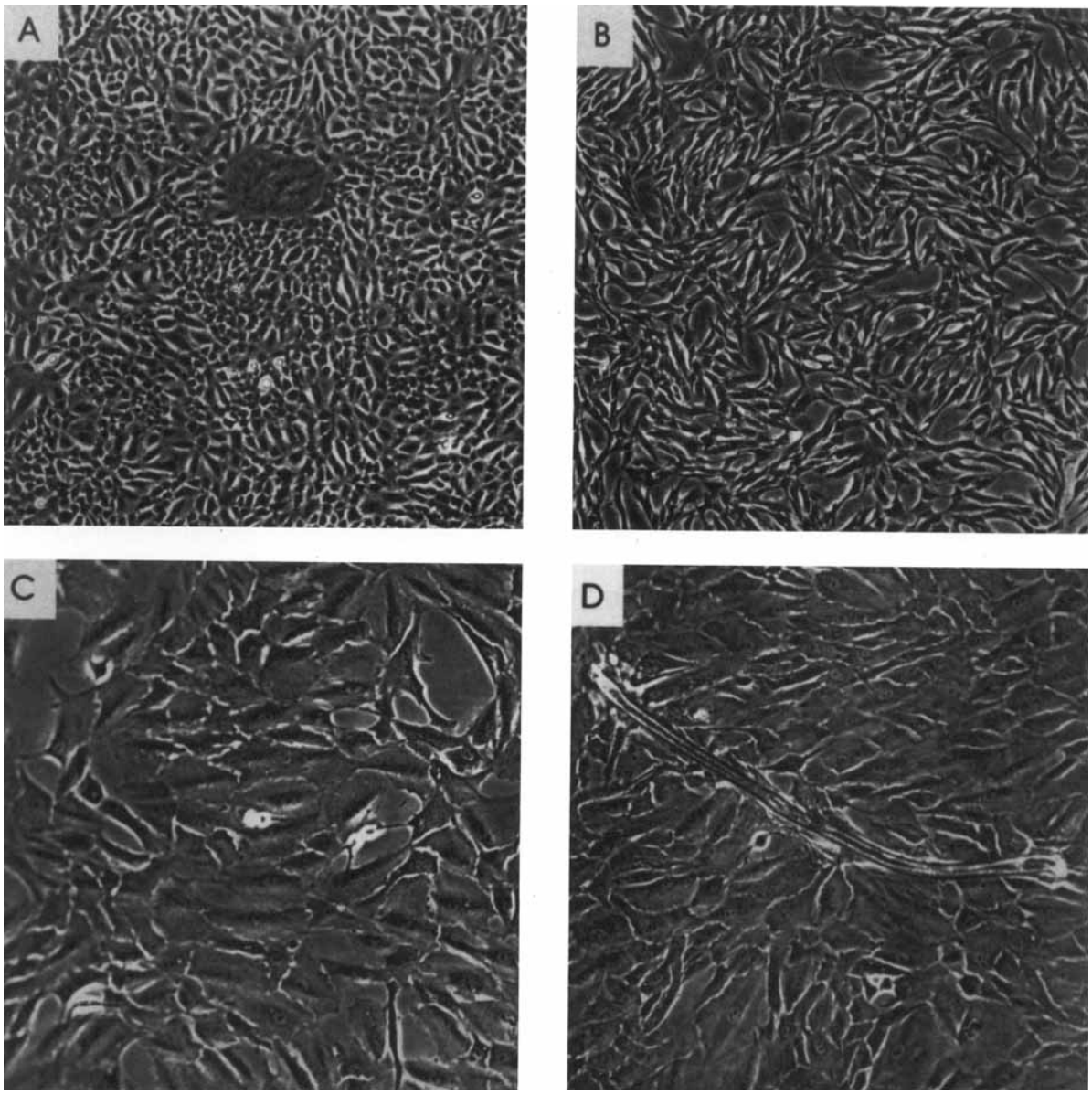

Fig. 1. Growth state related modifications in human microvascular endothelial cell (HMEC) morphology. Proliferative HMECs are characterized by a cobblestone morphology **(A)**, whereas predifferentiated HMECs assume a spindled phenotype **(B)**. Mitotic figures are noted within 24 h after HMEC transition from a predifferentiated to a proliferative growth state **(C)**. Spontaneous microtubule formation was noted in differentiated HMEC cultures **(D)**. HMECs were photographed: A = during proliferative growth (×100); B = after induction of predifferentiation via the low serum, 4 mM ethionine protocol (×100); C = following a 24 h culture in ethionine-free, complete medium after induction of predifferentiation (×250); D = during spontaneous differentiation (×250).

Several uniform findings, which were independent of the culture state of growth, were found during the analysis of the HPLC nucleotide profiles (Table I). As anticipated, due to its recognized position as the primary cellular energy reserve, ATP was the main high energy phosphate in all of the HMEC cultures. Further, all of the HMEC growth states possessed an energy charge (e.c. = [ATP] + ½ [ADP]/[ATP] + [ADP] + [AMP]) indicative of ongoing, active oxidative metabolism, i.e., 0.97, 0.93, 0.96, for the proliferative, predifferentiated, and differentiated HMECs, respectively. In addition, all of the HMEC cultures possessed a highly reduced redox poise, which is expressed as the ratio $NAD(P)H/NAD(P)^+$. The redox states were de-

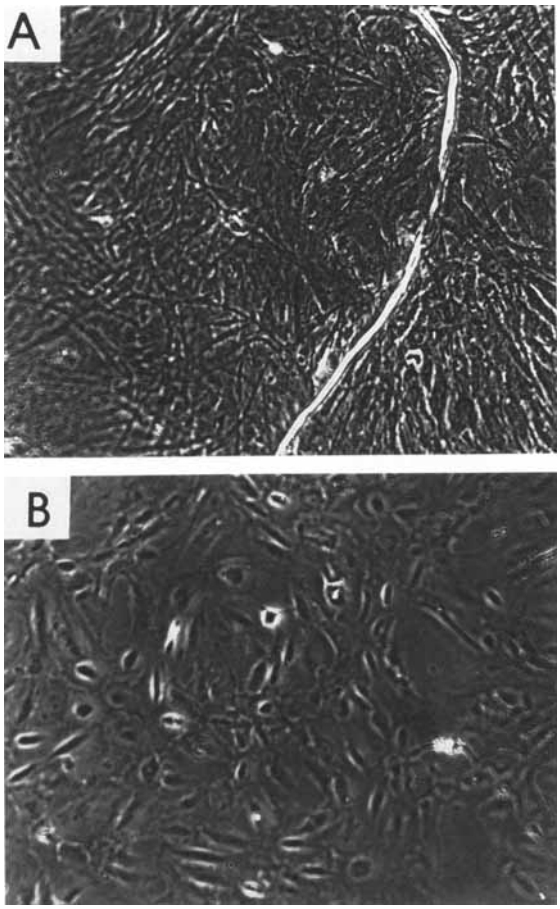

Fig. 2. Growth state reciprocity of human microvascular endothelial cells (HMECs). Within 24 h after passage to a noncontact inhibited growth state, mitotic figures were visible in the formerly differentiated HMEC cultures. HMECs were photographed: A = during spontaneous differentiation (×100); B = formerly differentiated cultures, 24 h after passage to a noncontact inhibited growth state (×100).

termined to be 0.90, 0.90, and 1.03 for the proliferative, differentiated, and predifferentiated cultures, respectively. Further, in all of the HMEC growth states, NADH was the primary form of reduced nicotinamide nucleotides.

However, in addition to these uniform nucleotide findings, other components of the HPLC nucleotide profiles demonstrated that there were also major bioenergetic differences. Further, this variation in nucleotide profiles was associated with the HMEC state of growth. Significantly increased levels of the high energy phosphates ATP, GTP, and UTP and CTP were detected in the proliferative HMEC cultures relative to levels detected in either the differentiated or predifferentiated HMECs (Table I). Further, proliferative HMECs possessed significantly higher levels of ADP and NADPH, relative to differentiated HMECs. Higher levels of total adenine nucleotides (AMP + ADP + ATP), total nicotinamide adenine dinucleotides (NAD^+ + NADH), and total nicotinamide adenine dinucleotide phosphates ($NADP^+$ + NADPH) were detected in proliferative HMECs relative to other growth states. In addition, predifferentiated HMECs were shown to contain nucleotide levels which were intermediate between those obtained from the proliferative and differentiated HMECs. These findings are consistent with the predifferentiated cellular phenotypic appearance and functional behavior [35].

Further, from a cellular biochemical perspective, both the processes of HMEC predifferentiation and differentiation were readily reversible. Within 48 h after culture in an ethionine free, rich medium (predifferentiated HMECs, n = 4), or passage to a noncontact inhibited growth state (differentiated HMECs, n = 4), cellular bioenergetic profiles and GSH status returned to levels detected in proliferative HMECs. These findings demonstrated that the HMECs' growth state reciprocity encompassed not only functional [35] and morphological aspects, but also cellular biochemical components.

Results of the HMEC GSH determinations showed that, like the cellular levels of high energy phosphates, HMEC GSH levels reflected the cellular state of growth. The highest levels of GSH were found in proliferative HMECs, while the intermediate and the lowest levels of GSH were present in the predifferentiated and differentiated cultures, respectively (Table I). Levels of GSSG were nondetectable (<0.01 nmol/ml) in all of the HMEC samples.

DISCUSSION

Novel information regarding endothelial cell biology is reported in this paper, in that we are the first group to characterize the bioenergetic status and GSH levels of human microvascular endothelial cells. Further, the results of this study demonstrate, for the first time, that as a component of their differentiated-proliferative growth state transition, HMECs significantly modify their morphology, bioenergetic profile and GSH status. While these findings are consistent with the predictable biochemical and morphological accommodations that would be requisite for HMEC re-entry into the cell cycle, the fact that these cellular modifications occur is indicative of the inherent plasticity present in

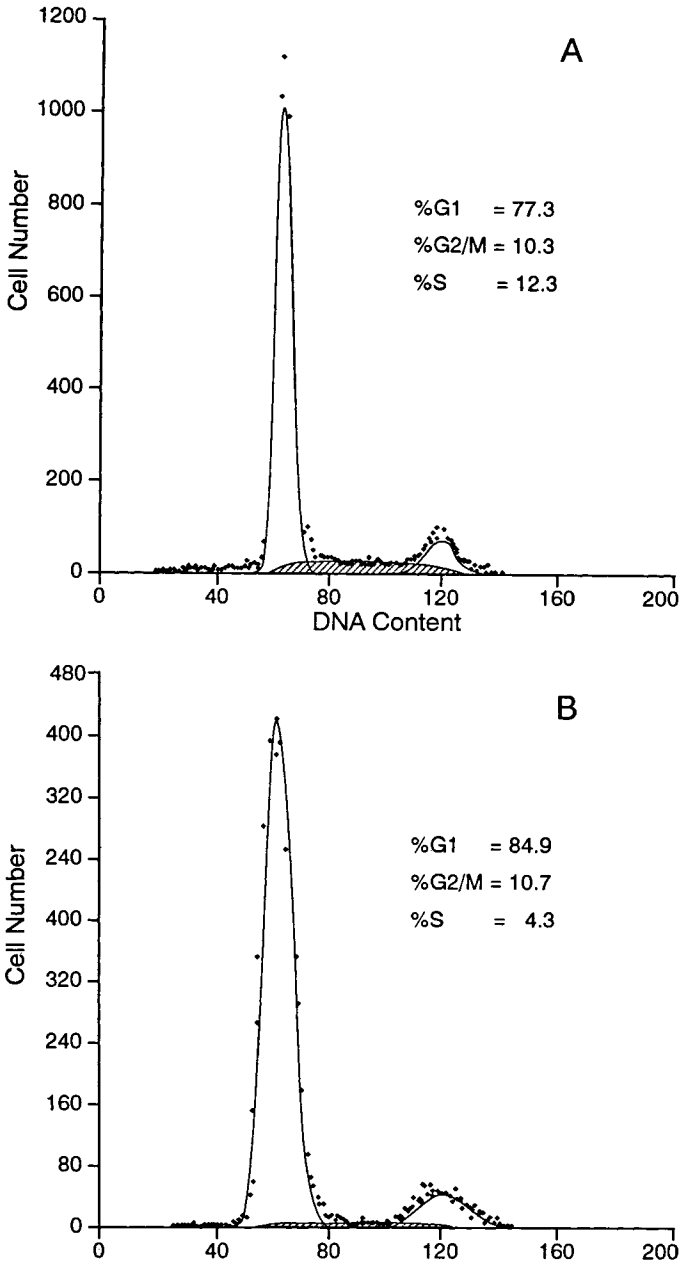

Fig. 3. Representative histograms of DNA-related fluorescence of propidium iodide stained human microvascular endothelial cell nuclei that were harvested: **A** = during proliferative growth; **B** = after spontaneous differentiation. Flow cytometry data cell cycle distributions were determined by utilization of the cell cycle analysis software MULTICYCLE, using a zero order (the most conservative exponential order) to determine the S phase compartment shape. The shaded area represents the S phase.

the HMEC phenotype. Further, by demonstrating this biochemical adaptability and environmental responsiveness, this study helps to clarify how HMECs manage to retain a growth state reciprocity.

The morphological changes observed in this study during the proliferative-differentiated growth transition are in agreement with alterations in cellular shape detected in previous endothelial cell studies [24,33,49]. Those prior studies, conducted in HMECs, human umbilical vein endothelial cells (HUVECs), and animal endothelial cells, demonstrated that similar cellular shape alterations, e.g., assumption of a spindled morphology, occurred during the induction of differentiation [24,33,49]. Our results, in

TABLE I. HPLC Nucleotide Analyses of Human Microvascular Endothelial Cells (HMECs) Assayed During the Following Growth States: Proliferative (PRO) n = 15, Predifferentiated (PRE) n = 8, Differentiated (DIF) n = 8†

Nucleotide	PRO	PRE	DIF
AMP	0.92 ± 0.44	0.88 ± 0.81	0.49 ± 0.29
ADP	2.37 ± 0.43*	2.32 ± 0.42	1.72 ± 0.15*
ATP	60.40 ± 3.55**	38.20 ± 9.52**	32.60 ± 5.01*
Total (ATP+ADP+AMP)	63.69	42.20	34.81
NAD+	8.79 ± 1.47	7.70 ± 1.96	5.72 ± 1.46
NADH	6.45 ± 1.29	6.61 ± 0.81	4.44 ± 1.10
Total (NAD^++NADH)	15.24	14.31	10.16
$NADP^+$	0.36 ± 0.11	0.44 ± 0.14	0.28 ± 0.11
NADPH	1.81 ± 0.45*	1.78 ± 0.35***	0.98 ± 0.19****
Total ($NADP^+$+NADPH)	2.17	2.22	1.26
GTP	8.72 ± 0.51******	6.39 ± 1.71*****	5.80 ± 1.02*
UTP & CTP	4.84 ± 0.34*****	3.29 ± 0.97****	3.10 ± 0.53*
GSH	66.5 ± 5.3***	52.2 ± 5.2*****	32.5 ± 3.8****

†HMEC glutathione (GSH) levels were determined by enzymatic analyses, n = 8 for each of the PRO, PRE, and DIF cultures. Statistical analyses were conducted with the Kruskal-Wallis one-way analysis of variance, followed by the Mann-Whitney U-test, *P <0.001, PRO vs. DIF; **P <0.001, PRO vs. PRE; ***P <0.001 PRE vs. DIF; ****P <0.002, PRO vs. PRE; *****P <0.02, PRO vs. PRE. Results are expressed as nmol/mg protein, $\bar{x}$ ± S.D.

conjunction with the previous reports, show that despite the intrinsic cellular differences attributable to the site of origin, both large vessel and small vessel endothelial cells manifest similar morphological changes during the induction of differentiation.

There are two probable, mutually inclusive, means by which the HMEC morphology was altered during the transition from proliferative to differentiated growth. The shape of anchorage dependent cells, such as HMECs, is primarily determined by the contributions of the intracellular cytoskeletal tensile forces in conjunction with the cellular-ECM interaction [1,23,26,28]. Both of these HMEC morphological determinants (cytoskeleton and ECM interaction) are likely to have been modified during the proliferative-differentiated growth state transition. The proliferative cytoskeletal configuration promotes a cobblestone, nonpolar phenotype which facilitates DNA uncoiling during the S phase [23,24]. In contrast, during differentiated growth, the HMEC cytoskeleton is modified to allow for a spindled shape [23,24].

We have previously shown that the induction of the process of HMEC differentiation is accompanied by modifications in the HMEC-integrin receptor expression and/or organization, and that these changes result in enhanced HMEC motility, augmentation of intercellular association, and accelerated microtubule formation [35]. To promote differentiation in our studies, HMECs were maintained, as confluent, contact inhibited cultures. During this time, there was ongoing autologous remodelling and replacement of the hFN with HMEC products such as laminin, collagen type IV, and heparin sulfate [4,15]. Therefore, upon achieving a state of differentiation, the initial hFN would have been significantly modified and therefore would more closely resemble the in vivo basement membrane of differentiated HMECs [4,15].

The analysis of the HMEC nucleotide profiles demonstrated that several uniform findings, which were independent of the culture growth state, were present. In all HMEC cultures, as is true in most cells, the majority of high energy phosphate was is the form of ATP [36]. In addition, all of the HMEC growth states possessed energy charges >0.90. These high energy levels are valid indicators that during culture HMECs maintain high rates of oxidative metabolism. Another consistent finding among the HMEC culture growth states was the presence of a highly reduced redox poise. It is improbable that this finding of reduced redox states in all of the HMEC culture groups reflects cellular hypoxia, or a cellular handling artifact. First, all three

culture groups were harvested under aerobic conditions. Also, during hypoxia, there would be a precipitous drop in cellular ATP levels as the cells shift to anaerobic metabolism [17,36]. However, as is evident by both the HMEC energy charges and the ATP levels, the cellular energy status was not perturbed during the HMEC harvesting for HPLC analysis. Therefore, it is proposed that the HMEC redox states reflect the effects of a mitochondrial state 4 stage of respiration. The ATP/ADP ratios obtained in the HMEC culture groups (PRO 25, PRE 16, DIF 19) suggest that ADP is a rate limiting substrate for HMEC respiration. Because both orthophosphate and ADP function to stimulate the activity of F_0F_1 ATP synthase, a relative deficit of mitochondrial ADP would perturb the mitochondrial proton gradient by depressing the activity of the proton gradient maintaining enzyme, F_0F_1 ATP synthase [36]. A decrease in the inner mitochondrial matrix proton gradient would delay the dissipation of the electron transport system's electrochemical gradient, impeding the mitochondrial electron transport, and ultimately resulting in an accumulation of reduced electron transport carriers, such as NADH [36]. A final uniform nucleotide finding noted in the HPLC analyses was that NADH was the primary form of reduced nicotinamide nucleotides. These results are consistent with the nicotinamide nucleotide distributions determined in other cells, and likely reflect a high rate of activity of the NAD linked dehydrogenases that are employed in the oxidative pathways of metabolism [17,25,36].

Although similarities in the HMEC nucleotide profiles were noted, there were also culture growth state related differences. Further, these growth state related nucleotide differences reflected the ongoing cellular biochemical adaptations that would enable HMECs to return to a proliferative growth state. The increased levels of ATP, GTP, and UTP, and CTP detected in the proliferative HMECs would be essential both to provide the additional energy necessary for DNA synthesis (ATP and GTP), and the nucleotide components for DNA [36,42]. Although the majority of high energy phosphates are maintained as the ribose moiety, due to ongoing DNA synthesis in the proliferative HMECs, the high energy nucleotide increases detected in the proliferative HMEC cultures undoubtedly have a deoxyribose component [36]. Proliferative HMEC cultures also possessed increased levels of NADPH. Because NADPH functions as the ultimate provider of reducing equivalents for an enzyme integral in DNA synthesis, ribonucleotide reductase, this finding is consistent with the return of HMECs to the cell cycle [10,21,22]. These increases in NADPH levels suggest that the hexose monophosphate shunt, which provides two components necessary for DNA synthesis, NADPH and ribose sugars, is stimulated in proliferative HMECs [36]. The proliferative HMEC cultures also possessed higher total levels of adenine nucleotides, nicotinamide adenine dinucleotides, and, relative to differentiated HMECs, higher levels of nicotinamide adenine dinucleotide phosphates. It is probable that these findings reflect both an increased nucleotide synthesis and turnover in the proliferative cultures [36].

The nucleotide profiles of the predifferentiated cultures were determined to be intermediate between those obtained for the proliferative or differentiated HMECs. Recently, we have reported that exposure to ethionine induces a morphological and functional state of predifferentiation in HMECs [35]. The current study substantiates our earlier findings by demonstrating that ethionine also induces a biochemical state of predifferentiation in HMECs. Further, the intermediate levels of ATP detected in the predifferentiated HMECs suggests that ethionine, like methionine, has the capacity to complex directly with cellular ATP [36].

The levels of ATP obtained in the predifferentiated and differentiated HMEC cultures compare favorably with results obtained from other studies [40,51]. Miura et al. [1992] reported ATP levels of 37.5 nmol/mg protein in HUVEs using the luciferase-luciferin chemiluminescence assay [40]. In addition, in a study designed to evaluate the effects of oxidants on endothelial cell permeability, Wilson et al. [1990] reported mean ATP levels of 34.9 nmol/mg protein (HPLC and luciferase methods) in porcine pulmonary artery endothelial cells [51]. Notably, the levels of ATP detected in our study for the proliferative HMECs, 60.40 ± 3.55, are markedly increased relative to values obtained in the Muira or Wilson studies. There are several reasons to account for these differences in results. First, both the porcine endothelial cells (species variation) and the HUVEs are endothelial cells obtained from large vessels. In addition, it is well accepted that there is a heterogeneity among endothelial cell populations that reflects not only

a species variation, but also differences attributable to the site of origin, e.g., comparison of the characteristics of endothelial cells obtained from large vessels vs. the microvasculature [4,12]. Further, because HUVEs are obtained from an end stage organ, it is probable, due to their imminent cessation of function, that HUVEs don't retain the capacity to readily revert from differentiated to proliferative growth. We maintain that the increased levels of ATP detected in proliferative HMECs reflect an inherent HMEC biochemical adaptability that is integral for these cells' retention of a growth state reciprocity.

Because there is a lack of information characterizing cellular bioenergetic status in human or animal endothelial cells, comparison of the HMEC nucleotide profiles with other endothelial cells' profiles is not feasible. However, previous studies have reported nucleotide content in freshly harvested animal tissues or cells [17,25]. The levels of nicotinamide adenine dinucleotides detected in this study are comparable to levels obtained by Kalhorn et al. [1985] in rat hepatic tissue [25]. However, as would be anticipated, due to the participation of the liver in fatty acid synthesis and lipogenesis, the levels of NADPH obtained were higher in Kalhorn's study [25,36]. Geisbuhler et al. [1984] reported bioenergetic profiles in rat cardiac myocytes [17]. Although the HMEC nucleotide levels were in the same range as myocyte profiles, there were marked, but not unexpected, differences in comparison of the nucleotide profiles between the HMECs and the myocytes; HMECs contained appreciably higher levels of ATP, GTP, UTP, and NADH [17]. Because rat cardiac myocytes are terminally differentiated, these differences may reflect both a species and cellular variation.

As would be anticipated, in non-oxidant stressed cells, the levels of GSSG remained nondetectable in all HMEC cultures [38,39]. The levels of GSH detected in human HMECs in this study are comparable, but slightly higher, to reported GSH levels found in other human cells [34,40]. Recently, in a study designed to investigate the effect of cystine uptake on GSH levels, Miura et al. [1992] reported that HUVE levels of GSH ranged from 35 to 45 nmol GSH/mg protein in nontreated cultures [40]. Our mean levels of GSH ranged from 32.45 to 66.52 nmol/mg protein in differentiated and proliferative cultures, respectively. In this study, the highest levels of GSH were detected in HMECs that were in a state of proliferative growth. This finding is consistent with previous publications which have reported cell cycle related increases in cellular GSH levels [6,19,30,34,45]. Although the differentiated HMEC GSH levels are in a range comparable to other endothelial cells, and therefore probably adequate for cytoprotection, during proliferative growth there are additional cellular physiological demands [40,42]. Therefore, the additional reducing equivalents provided by GSH (both as GSH and glutaredoxin) would be advantageous in maintaining the activities of two thiol dependent enzymes integral for DNA synthesis, DNA polymerase alpha, and ribonucleotide reductase [10,16,21,22].

The results of this study demonstrate that the HMEC biochemical plasticity is one of the adaptations that enable HMECs to retain a growth state reciprocity. Our findings also demonstrate that HMECs, especially during the proliferative growth state, are biochemically distinct from endothelial cells harvested from large vessels. Because of the unique physiological demands placed upon microvascular endothelial cells, these findings are not unanticipated [12,27,32]. In conclusion, our results show that HMECS have a growth state responsive biochemical phenotype, and suggest that HMECs, due to their unique cellular features and functions, are the indicated cells to employ when studying diseases that affect the human microvasculature.

ACKNOWLEDGMENTS

This study was supported in part by NIH/NHLB RO1 HL48547.

REFERENCES

1. Albelda SM, Buck CA (1990): Integrins and other cell adhesion molecules. FASEB J 4:2868–2880.
2. Beilke MA (1989): Vascular endothelium in immunology and infectious disease. Rev Infect Dis 11:273–283.
3. Beitz JG, Kim IS, Calabresi P, Frackelton AR, Jr (1991): Human microvascular endothelial cells express receptors for platelet-derived growth factor. Proc Natl Acad Sci USA 88:2021–2125.
4. Belloni PN, Tressler RJ (1990): Microvascular endothelial cell heterogeneity: interactions with leukocytes and tumor cells. Cancer Metastasis Rev 8:353–398.
5. Bevilacqua MP, Stenglin S, Gimbrone MA, Seed B (1989): Endothelial leukocyte adhesion molecule 1: receptor for neutrophils related to complement regulatory proteins and lectins. Science 243:1160–1165.
6. Butler JD, Key JD, Hughes BF, Tietze F, Raiford DS, Reed GF, Brannon PM, Speilberg SP, Schulman JD (1987): Glutathione metabolism in normal and cystinotic fibroblasts. Exp Cell Res 172:158–167.
7. Campochiaro PA, Jerdan JA, Glaser BM (1986): The extracellular matrix of human retinal pigmented epithelial cells in vivo and its synthesis in vitro. Invest Ophthalmol Vis Sci 27:1615–1619.

8. Chung-Welch N, Patton WF, Yen-Patton GPA, Hechtman HB, Shepro D (1989): Phenotypic comparison between mesothelial and microvascular endothelial cell lineages using conventional endothelial cell markers, cytoskeletal protein markers and in vitro assays of angiogenic potential. Differentiation 42:44–53.
9. Dorvini-Zis K, Prameya R, Bowman PD (1991): Culture and characterization of microvascular endothelial cells from human brain. Lab Invest 64:425–436.
10. Engstrom Y, Eriksson S, Jildevik I, Skog S, Thelander L, Tribukait B (1985): Cell cycle dependent expression of mammalian ribonucleotide reductase. J Biol Chem 260:9114–9116.
11. Eyer P, Podhradsky D (1986): Evaluation of the micromethod for determination of glutathione using enzymatic cycling and Ellman's reagent. Anal Biochem 153: 57–66.
12. Fajardo LF (1989): The complexity of endothelial cells. Am J Clin Pathol 92:241–250.
13. Fawcett J, Harris AL, Bicknell R (1991): Isolation and properties in culture of human adrenal capillary endothelial cells. Biochem Biophys Res Commun 174:903–908.
14. Folkman J, Klagsbrun M (1987): Angiogenic factors. Science 235:442–447.
15. Folkman J, Shing Y (1992): Angiogenesis. J Biol Chem 267:10931–10934.
16. Foster KA, Collins JM (1985): The interrelation between DNA synthesis rates and DNA polymerases bound to the nuclear matrix in synchronized HeLa cells. J Biol Chem 260:4229–4235.
17. Geisbuhler T, Altschuld RA, Trewyn RW, Ansel AJ, Lanka K, Brierley GP (1984): Adenine nucleotide metabolism and compartmentalization in isolated adult rat heart cells. Circ Res 54:536–546.
18. Harsem E, DeTombe PP, DeJong JW (1982): Simultaneous determination of myocardial adenine nucleotides and creatine phosphate by high-performance liquid chromatography. J Chromatogr 230:131–136.
19. Harris JW, Teng SS (1972): Sulfhydryl groups during the S phase: comparison of cells from G1, plateau-phase G1, and G0. Cell Physiol 81:91–96.
20. Hohl CM, Wimsatt DK, Brierley GP, Altschuld RA (1989): IMP production by ATP-depleted adult rat heart cells. Circ Res 65:754–760.
21. Holmgren A (1979): Glutathione-dependent synthesis of deoxyribonucleotides. J Biol Chem 254:3664–3678.
22. Holmgren A (1981): Regulation of ribonucleotide reductase. Curr Top Cell Regul 19:47–76.
23. Ingber DE (1990): Fibronectin controls capillary endothelial cell growth by modulating cell shape. Proc Natl Acad Sci USA 87:3579–3583.
24. Ingber DE, Folkman J (1989): Mechanochemical switching between growth and differentiation during fibroblast growth factor-stimulated angiogenesis in vitro: role of extracellular matrix. J Cell Biol 109:317–330.
25. Kalhorn TF, Thummel KE, Nelson SD, Slattery JT (1985): Analysis of oxidized and reduced pyridine dinucleotides in rat liver by high performance liquid chromatography. Anal Biochem 151:343–347.
26. Katz AM, Rosenthal D, Sauder DN (1991): Cell adhesion molecules: structure, function, and implication in a variety of cutaneous and other pathologic conditions. Int J Dermatol 30:153–160.
27. Klagsbrun M, D'Amore PA (1991): Regulators of angiogenesis. Annu Rev Physiol 53:217–239.
28. Kramer RH, Cheng YF, Clyman R (1990): Human microvascular endothelial cells use B1 and B3 integrin receptor complexes to attach to laminin. J Cell Biol 111:1233–1243.
29. Lantry LE, Fryczkowski AW, Mallery SR, Sadoun ET, Titterington LC, Thio D, Stephens RE: Isolation of novel microvascular endothelial cells from the choriocapillaris of the human eyes. Submitted: Exp Eye Res.
30. Lee FYF, Siemann DW, Allalunis-Turner MJ, Keng PC (1988): Glutathione contents in human and rodent tumor cells in various phases of the cell cycle. Cancer Res 48:3661–3665.
31. Lowry OH, Rosebrough NJ, Farr AL, Randall RJ (1951): Protein measurement with the Folin phenol reagent. J Biol Chem 193:265–275.
32. Maciag T (1990): Molecular and Cellular Mechanisms of Angiogenesis. In Richardson J (ed): "Important Advances in Oncology." Philadelphia: JB Lippincott, pp 85–98.
33. Maciag T, Kadish J, Wilkins L, Stemerman MB, Weinstein R (1982): Organizational behavior of human umbilical vein endothelial cells. J Cell Biol 94:511–520.
34. Mallery SR, Laufman HB, Solt CW, Stephens RE (1991): Association of cellular thiol redox status with mitogen-induced calcium mobilization and cell cycle progression in human fibroblasts. J Cell Biochem 45:82–92.
35. Mallery SR, Lantry LE, Laufman HB, Brierley GP, Stephens RE: Induction of a morphological and functional state of pre-differentiation in human microvascular endothelial cells after exposure to ethionine. Submitted:Differentiation.
36. Matthews CK, van Holde KE (1990): "Biochemistry." Redwood City, CA: Benjamin/Cummings Publishing Co., pp 85, 493–501, 712–713, 861–863.
37. Mbemba FA, Houbion A, Paes M, Remacle J (1985): Subcellular localization and modification with ageing of glutathione, glutathione peroxidase and glutathione reductase activities in human fibroblasts. Biochim Biophys Acta 838:211–220.
38. Meister A (1988): Glutathione metabolism and its selective modification. J Biol Chem 263:17205–17208.
39. Meister A, Anderson ME (1983): Glutathione. Annu Rev Biochem 52:711–760.
40. Miura K, Ishii T, Sugita Y, Bannai S (1992): Cystine uptake and glutathione levels in endothelial cells exposed to oxidative stress. Am J Physiol 262:C50–C58.
41. Oshino N, Chance B (1977): Properties of glutathione release observed during reduction of organic hydroperoxide, dimethylation of aminopyrine, and oxidation of some substances in perfused rat liver, and their implications for the physiological function of catalase. Biochem J 162:509–525.
42. Pardee AB (1989): G1 events and regulation of cell proliferation. Science 246:603–608.
43. Pober JS, Doukas J, Hughes CCW, Savage COS, Munro M, Cotran RS (1990): The potential roles of vascular endothelium in immune reactions. Hum Immunol 28: 258–262.
44. Pollack A (1990): Flow cytometric cell-kinetic analysis by simultaneously staining nuclei with propidium iodide and fluorescein isothiocyanate. Methods Cell Biol 33:315–323.

45. Shaw JP, Chou IN (1986): Elevation of intracellular glutathione content associated with mitogenic stimulation of quiescent fibroblasts. J Cell Physiol 129:193–198.
46. Springer TA (1990): Adhesion receptors of the immune system. Nature 346:425–434.
47. Tooke JE (1989): Microcirculation and diabetes. Br Med Bull 45:206–223.
48. Vane JR, Anggard EE, Botting RM (1990): Regulatory functions of the endothelium. N Engl J Med 323:27–36.
49. van Hinsbergh VWM, Mommaas-Keinhuis AM, Weinstein R, Maciag T (1986): Propagation and morphologic phenotypes of human umbilical cord artery endothelial cells. Eur J Cell Biol 42:101–112.
50. Voyta JC, Via DP, Butterfield CE, Zetter BR (1984): Identification and isolation of endothelial cells based on their increased uptake of acetylated-low density lipoprotein. J Cell Biol 99:2034–2040.
51. Wilson J, Winter M, Shasby DM (1990): Oxidants, ATP depletion, and endothelial permeability to macromolecules. Blood 76:2578–2582.